PERGAMON

Journal of the Mechanics and Physics of Solids
50 (2002) 1079–1098

JOURNAL OF THE
MECHANICS AND
PHYSICS OF SOLIDS

www.elsevier.com/locate/jmps

Plastic ratcheting induced cracks in thin film structures

M. Huang[a,1], Z. Suo[a,*], Q. Ma[b]

[a] *Mechanical and Aerospace Engineering Department, Princeton Materials Institute, Princeton University, P.O. Box CN5263, Princeton, NJ 08544-5263, USA*
[b] *Intel Corporation, 2200 Mission College Blvd., Santa Clara, CA 95052, USA*

Received 25 May 2001; accepted 18 August 2001

Abstract

In the microelectronic and photonic industries, temperature cycling has long been used as a reliability test to qualify integrated materials structures of small feature sizes. The test is time consuming, and is a bottleneck for innovation. Tremendous needs exist to understand various failure modes in the integrated structures caused by cyclic temperatures. This paper presents a systematic study of a failure mechanism recently discovered by the authors. In a thin film structure comprising both ductile and brittle materials, the thermal expansion mismatch can cause the ductile material to plastically yield in every temperature cycle. Under certain circumstances, the plastic deformation ratchets, namely, accumulates in the same direction as the temperature cycles. The ratcheting deformation in the ductile material may build up stress in the brittle materials, leading to cracking. The paper introduces an analogy between ratcheting and viscous flow. An analytical model is developed, which explains the experimental observations, and allows one to design the structure to avert this failure mode. Design rules with increasing levels of sophistication are described. Concepts presented here are generic to related phenomena in thin film structures.

Keywords: Temperature cycling; Plasticity; Thin films; Ratcheting; Cracking

1. Introduction

Temperature cycling is widely used in the industry to qualify integrated small structures of dissimilar materials. After being cycled between two temperatures for hundreds and thousands of times, a structure is sectioned and examined in microscopes

* Corresponding author. Tel.: +1-609-258-0250; fax: +1-609-258-5877.
E-mail address: suo@princeton.edu (Z. Suo).
[1] Current address: Lightcross Inc., 2630 Corporate Place, Monteray Park, CA 91754, USA.

0022-5096/02/$ - see front matter
PII: S0022-5096(01)00113-2

for failure (e.g., distortion and cracking). If a failure mode is found, modifications are made in the next iteration of the structure by changing either materials, geometries, or processing parameters. The modified structure is temperature cycled again, followed by the microscopy examination. The iterations do not guarantee convergence, as the modifications made to avert one failure mode may cause another failure mode. These make-and-break iterations are extremely time consuming, and are a bottleneck for innovation. Consequently, it is imperative to understand various failure modes caused by temperature cycling. Such understanding would greatly impact the microelectronic, photonic and MEMS industries, where complex structures of small feature sizes are made, and miniaturalization and novel functionality demand new structures to be qualified rapidly. This paper systematically examines a failure mode recently discovered by the authors (Huang et al., 2000).

Fig. 1a illustrates a flip-chip package. A silicon die is bonded to a packaging substrate, with the interconnect structure facing the packaging substrate. Between the die and the substrate are layers of polymers (epoxy underfill and polyimide) and solder bumps. Fig. 1b details the left corner of the die. Illustrated is a metal (aluminum or copper) film of the top level interconnects on a dielectric (silica), with a silicon nitride (SiN) passivation film covering the metal film and silica. The SiN film is deposited over the interconnect structure before the die is bonded to the packaging substrate. Since the packaging substrate has a larger thermal expansion coefficient than the silicon die, upon cooling from the curing temperature, a shear stress τ_0 develops on the silicon die, pointing toward the die center (Alpern et al., 1994; Nguyen et al., 1995; Liu et al., 1999). Leading failure modes in the flip-chip package caused by temperature cycling include die–polymer or polymer–substrate debonding (Yan and Agarwal, 1998; Gurumurthy et al., 1998), solder bump detachment (Lau et al., 1998), metal film crawling (Huang et al., 2001a; Alpern et al., 1994; Isagawa et al., 1980; Thomas, 1985), and SiN film cracking (Huang et al., 2000; Michaelides and Sitaraman, 1999; Edwards et al., 1987; Alpern et al., 1994; Nguyen et al., 1995; Pendse, 1991, Gee et al., 1995). This paper focuses on SiN film cracking.

Fig. 1c is a schematic plan view of the die surface near a corner. Plan view micrographs of several interconnect test structures are shown in Fig. 2. The exact testing conditions are unavailable to us, but the observations are generic. After about 1000 cycles between -55°C and $+125^{\circ}$C, the packaging substrate and the polymers are removed to expose the die surface. Cracks are observed in the SiN film over the metal film. The main experimental observations are as follows.

- Cracking occurs in the SiN film at the die corners.
- Cracking occurs after temperature cycles, and becomes more extensive as the number of cycles increases.
- Cracking occurs in the SiN film over the metal films, but not in the SiN film over silica.
- Cracking is more likely when the metal films are wide and the SiN film is thin.

Passivation film cracking has been observed for many years (Michaelides and Sitaraman, 1999; Edwards et al., 1987; Alpern et al., 1994; Nguyen et al., 1995; Pendse, 1991, Gee et al., 1995). Two questions have been intriguing. Why should cracks occur

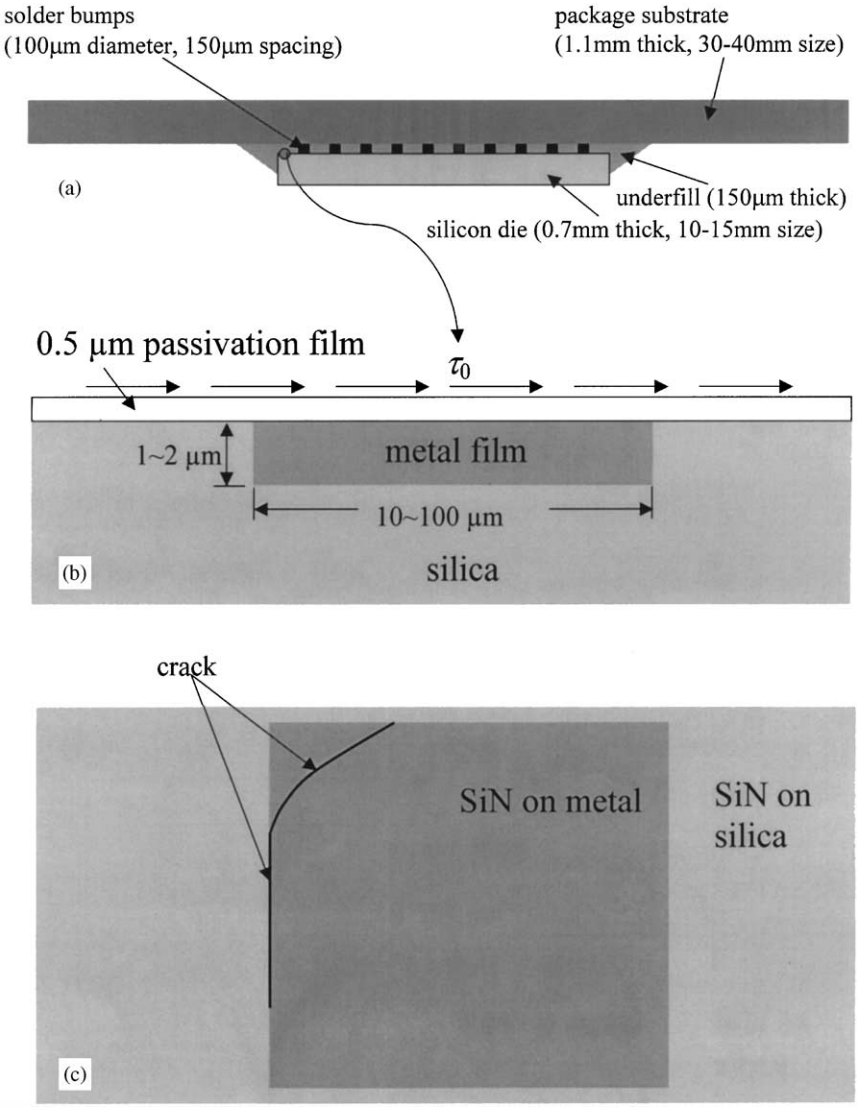

Fig. 1. (a) Flip-chip structure. (b) Magnified view of the left corner of the silicon die. (c) Schematic of a crack developed in the passivation film over the metal film.

after many temperature cycles? SiN does not have an intrinsic fatigue mechanism. Why should cracks occur at all? The shear stress on the die is transmitted through the polymers, and is limited by the yield strength of the polymers, say 100 MPa. The yield strength of the metal film exceeds 100 MPa (Nix, 1989). The fracture strength of the SiN thin film is on the order 1 GPa (Ma et al., 1998).

We have recently discovered a mechanism that answers these questions (Huang et al., 2000). As mentioned before, the thermal expansion coefficient of the silicon die is

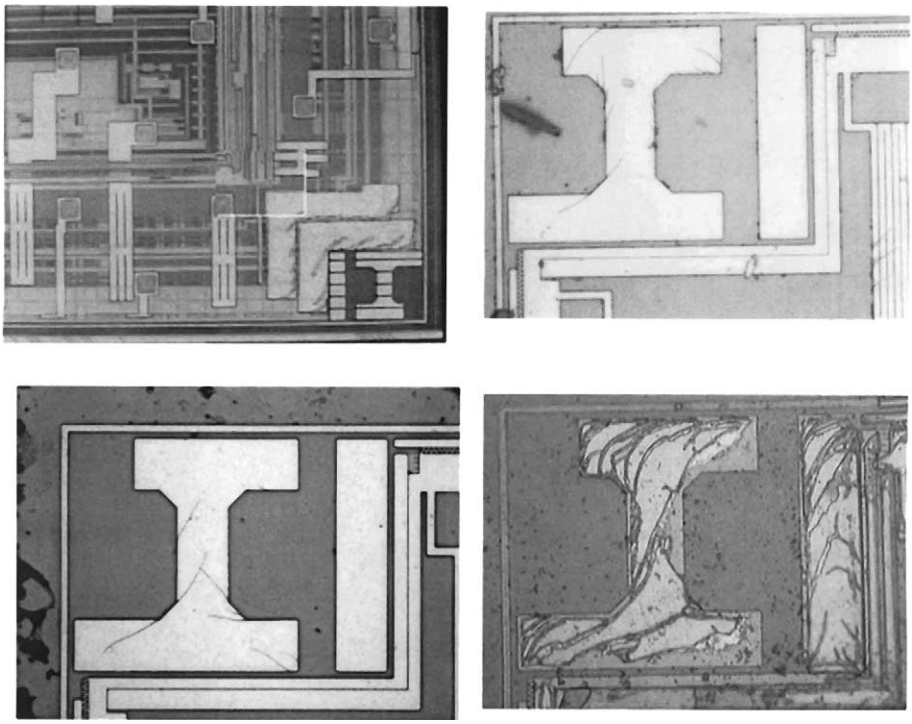

Fig. 2. Plan view micrographs of several interconnect test structures. The lighter region corresponds to aluminum film, and the darker region corresponds to silica dielectric. The entire surface is covered by a thin SiN film. Cracks are observed in SiN over the aluminum film after many temperature cycles.

much lower than that of the packaging substrate. The differential thermal expansion induces the shear stress, τ_0, at the die corners upon cooling from the curing temperature (Fig. 1b). When the temperature cycles in a range below the curing temperature, the shear stress τ_0 always points toward the center of the die. The shear stress τ_0 is partly sustained by a membrane stress σ in the passivation film, and partly transmitted to the metal film underneath as a shear stress in the metal, τ_m. The metal film also has a large thermal expansion mismatch with silicon and silica beneath, so that the metal film plastically yields in every temperature cycle. When the metal yields, the small shear stress in the metal, τ_m, will cause the metal to deform in shear plastically. The in-plane plastic strain in the metal film is constrained by the elastic substrate. Consequently, the amount of plastic shear strain increment per cycle in the metal is small, as will become evident later when we look at the model closely. The increment of the shear strain is in the same direction as the shear stress on the passivation film τ_0, which is always in the same direction during the temperature cycling. Incrementally, the shear stress in the metal film τ_m relaxes, and the membrane stress σ in the overlaying silicon nitride film builds up. It is this evolving stress state that cracks the SiN film after some cycles.

The deformation in the same direction caused by a cyclic load (temperature change in this case) is known as ratcheting deformation (Bree, 1967; Suresh, 1998; Jansson and Leckie, 1992). Several examples of ratcheting in thin film structures have been discovered recently (Begley and Evans, 2001; He et al., 2000; Huang et al., 2000, 2001a; Karlsson and Evans, 2001). As it turns out, these examples can all be understood in terms of a ratcheting-creep analogy to be introduced in this paper.

Huang et al. (2000) analyzed a plane strain model of passivation film cracking. The finite element method was used to evolve the stress field incrementally as the temperature changes. After many temperature cycles, the structure reached a steady state, in which the stress field in the passivation film remained unchanged and the metal film underwent cyclic plastic deformation upon further temperature cycling. In this paper, we will address two important issues that we could not address in the previous paper. First, in the previous paper, to limit the amount of computation, we assigned a low metal yield strength, so that the number of cycles needed to approach the steady state is limited below about 100. Second, to avert cracking, an industrial practice is to change the shape and size of the metal film. Consequently, to aid the industrial practice, we would like to do calculations over thousands of temperature cycles, for three-dimensional structures, and for many geometrical designs. Direct finite element calculation would require too much time to be practical.

This paper will develop analytical methods to circumvent these difficulties. The plan of the paper is as follows. Section 2 reviews the model of crawling of a blanket metal film, and introduces the concept of ratcheting-viscosity. In Section 3, a ratcheting-creep analogy is developed to analyze the evolving stress field in the passivation film as the metal film ratchets. Section 4 extends the ideas into a two-dimensional model to evolve stress field in a passivation film over a metal film of an arbitrary shape. As will be shown later, the normal stresses in the passivation film build up during temperature cycling, and reach the maximum value at the steady state. The steady state corresponds to a plane stress field, which can be rapidly determined by using a commercial finite element package.

2. Crawling of a blanket film on a semi-infinite substrate

Metal films near a die corner are sometimes observed to crawl toward the die center during temperature cycling (Alpern et al., 1994; Isagawa et al., 1980; Thomas, 1985). Such crawling breaks passivation films, and may even break thin metal lines themselves by excessive distortion (J.B. Han, private communication). Huang et al. (2001a) have developed an idealized model to study this phenomenon. This section casts the key results in a form useful for the present work. Fig. 3a illustrates a blanket metal film bonded on a semi-infinite elastic substrate. Throughout the paper, the metal is taken to be elastic and perfectly plastic, with an yield strength independent of the temperature within the range of the temperature cycling. Cycle the structure between temperatures T_L and T_H. At any given time, the whole structure is taken to have a uniform temperature. The effect of non-uniform temperature will not be studied in this paper. A shear stress, τ_m, acts on the surface of the metal film. For the time being, this

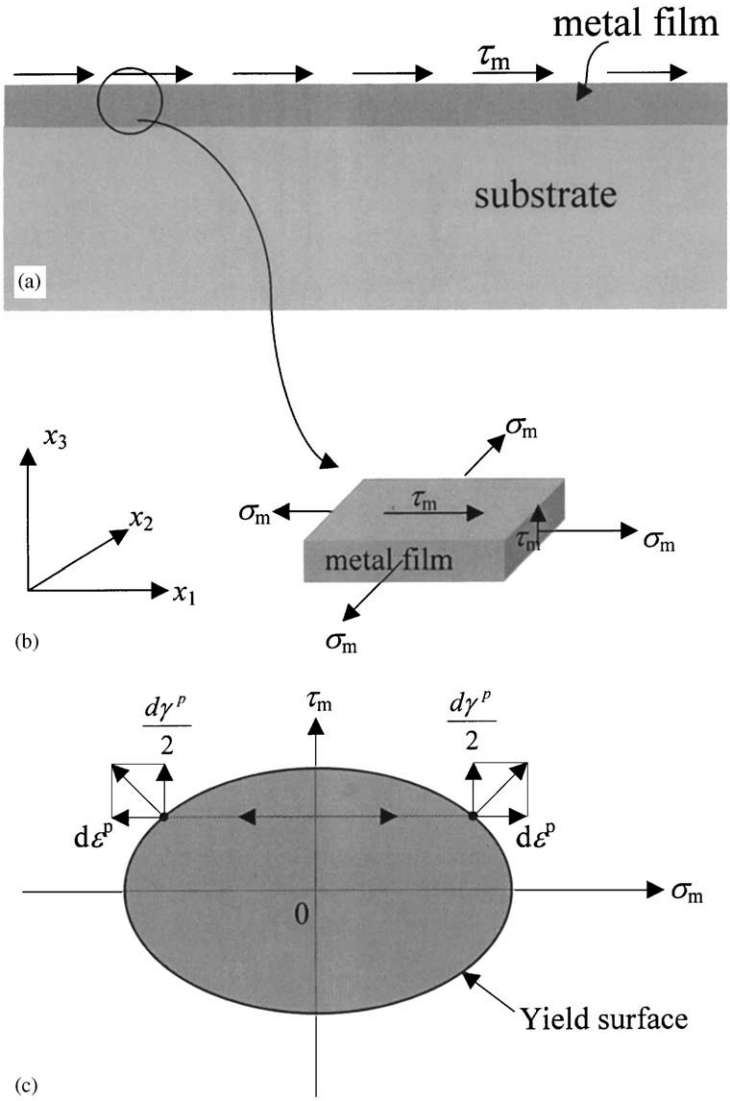

Fig. 3. (a) A magnified view of the left corner of the silicon die, showing the shear stress on the metal film. (b) The stress state in the film. (c) The yield surface.

shear stress is taken to be spatially uniform, and remains constant as the temperature cycles.

Under these assumptions, the stress field in the structure is very simple. The semi-infinite substrate is subject to the same shear stress τ_m, but no other stress components. Let the coordinates in the plane of the film be x_1 and x_2, the coordinate normal to the plane be x_3, and the coordinate x_1 coincide with the direction of the shear stress τ_m.

As shown in Fig. 3b, the film is in a uniform stress state of a combination of a biaxial stress and a shear stress:

$$\sigma_{11} = \sigma_{22} = \sigma_m, \quad \sigma_{13} = \tau_m, \quad \sigma_{23} = \sigma_{12} = 0. \tag{1}$$

The biaxial stress σ_m changes with the temperature. Obviously, the uniform stress states in the substrate and in the film satisfy the equilibrium conditions.

We next consider deformation compatibility between the film and the substrate. Let α_m and α_s be the thermal expansion coefficients of the metal film and the substrate ($\alpha_m > \alpha_s$). The semi-infinite substrate is not under in-plane stress. Consequently, when the temperature changes by dT, the in-plane strain of the substrate changes by $\alpha_s\, dT$. The reference state is the state before temperature cycling. Since the film is bonded to the substrate, the in-plane strain increment of the film equals that of the substrate, namely,

$$d\varepsilon^p + d\varepsilon^e + \alpha_m\, dT = \alpha_s\, dT, \tag{2}$$

where ε^p and ε^e are the plastic and the elastic in-plane strain in the metal film. That is, the thermal expansion mismatch between the metal film and the substrate is accommodated by a combination of elastic and plastic strains in the film.

We now consider material laws. The elastic in-plane strain relates to the biaxial stress in the film by Hooke's law:

$$d\varepsilon^e = \frac{1 - \nu_m}{E_m}\, d\sigma_m, \tag{3}$$

where E_m is Young's modulus and ν_m is Poisson's ratio of the film. The elastic shear strain in the film is given by

$$\gamma^e = \frac{2(1 + \nu_m)}{E_m}\tau_m. \tag{4}$$

When the film is elastic, $d\varepsilon^p = 0$, and the thermal mismatch is entirely accommodated by the elastic strain in the film. A combination of Eqs. (2) and (3) gives the biaxial stress increment

$$d\sigma_m = -\frac{E_m}{1 - \nu_m}(\alpha_m - \alpha_s)\, dT. \tag{5}$$

When the film is elastic, the biaxial stress increases as the temperature decreases.

When the film is plastic, $d\varepsilon^p \neq 0$. We adopt the J_2 flow theory (Hill, 1950). The deviatoric stress tensor, $s_{ij} = \sigma_{ij} - \sigma_{kk}\delta_{ij}/3$, has the components

$$s_{11} = s_{22} = \sigma_m/3, \quad s_{33} = -2\sigma_m/3, \quad s_{13} = \tau_m, \quad s_{23} = s_{12} = 0. \tag{6}$$

For simplicity, we assume that the metal is elastic and perfectly plastic. The uniaxial yield strength of the metal, Y, is constant and independent of the temperature and the amount of the plastic strain. The Mises yield condition, $3s_{ij}s_{ij}/2 = Y^2$, is specialized to

$$\sigma_m^2 + 3\tau_m^2 = Y^2. \tag{7}$$

The yield condition is an ellipse on the (σ_m, τ_m) plane (Fig. 3c). The metal film is elastic when the stress state is inside the ellipse, and yields when the stress state is on the ellipse. The stress state outside the ellipse cannot be attained by the metal. When the film yields, for a given τ_m, the biaxial stress can only be at one of the two levels:

$$\sigma_m = \pm \sqrt{Y^2 - 3\tau_m^2}. \tag{8}$$

These two stress states, tensile and compressive, are indicated in Fig. 3c.

The J_2 flow theory dictates that the plastic strain increment tensor is in the same direction as the deviatoric stress tensor, namely, $d\varepsilon_{ij} = s_{ij}^p \, d\lambda$, where $d\lambda$ is a scalar. Consequently, from Eq. (6) we obtain that

$$\frac{d\varepsilon^p}{\sigma_m/3} = \frac{d\gamma^p}{2\tau_m}, \tag{9}$$

where $\gamma^p = 2\varepsilon_{13}^p$ is the plastic shear strain in the film. Eq. (9) is the key to the understanding of metal film crawling. Its geometric interpretation is well known: the increment of the plastic strain tensor points in the direction normal to the yield surface (Fig. 3c). During plastic deformation, $d\varepsilon^p$ has the same sign as the biaxial stress σ_m, and $d\gamma^p$ has the same sign as the shear stress τ_m. When the temperature rises to yield the film in compression ($\sigma_m < 0$), the plastic in-plane strain decreases, $d\varepsilon^p < 0$. When the temperature drops to yield the film in tension ($\sigma_m > 0$), the plastic in-plane strain increases, $d\varepsilon^p > 0$. Since the film is bonded to the substrate, for a given temperature increment, $d\varepsilon^p$ is always finite. Consequently, in each cycle, γ^p increases by a finite amount in the direction of τ_m, both when the film is in tension *and* in compression. It is this feature that causes the film to crawl in the same direction as the temperature cycles.

During metal film yielding, $d\sigma_m = 0$ and $d\varepsilon^e = 0$. For a given temperature increment dT, Eq. (2) gives the increment of the plastic in-plane strain

$$d\varepsilon^p = -(\alpha_m - \alpha_s)\, dT. \tag{10}$$

The plastic in-plane strain increment in the film equals the thermal misfit strain increment. Substituting Eq. (10) into the J_2 flow rule, Eq. (9), gives the increment of the plastic shear strain

$$d\gamma^p = -\frac{6\tau_m}{\sigma_m}(\alpha_m - \alpha_s)\, dT. \tag{11}$$

When the film plastically deforms in tension, $\sigma_m = +\sqrt{Y^2 - 3\tau_m^2}$ and $dT < 0$. When the film plastically deforms in compression, $\sigma_m = -\sqrt{Y^2 - 3\tau_m^2}$ and $dT > 0$. In either case, the plastic shear strain increment is in the same direction of τ_m, namely, $d\gamma^p > 0$, giving rise to crawling. Fig. 4a shows the prescribed temperature change with time. Fig. 4b shows the plastic shear strain as a function of the temperature. The plastic shear strain remains constant when the metal film is elastic, and increases when the metal film is plastic.

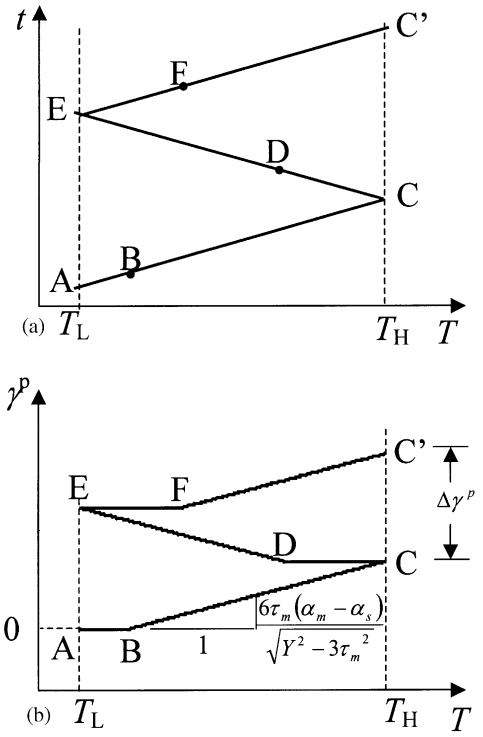

Fig. 4. (a) The prescribed temperature changes with time. (b) The plastic shear strain as a function of the temperature.

The ratcheting strain rate (i.e. the plastic shear strain increment per temperature cycle) can be obtained by using Eq. (11) and following through a cycle (CDEFC' in Fig. 4):

$$\Delta\gamma^{\mathrm{p}} = \frac{12(1-\nu_{\mathrm{m}})\tau_{\mathrm{m}}}{E_{\mathrm{m}}}\left[\frac{E_{\mathrm{m}}(\alpha_{\mathrm{m}}-\alpha_{\mathrm{s}})(T_{\mathrm{H}}-T_{\mathrm{L}})}{(1-\nu_{\mathrm{m}})\sqrt{Y^2-3\tau_{\mathrm{m}}^2}}-2\right]. \tag{12}$$

Fig. 5 plots the ratcheting strain rate, $\Delta\gamma^{\mathrm{p}}$, as a function of the shear stress, τ_{m}. We make an analogy between the strain *per temperature cycle* (i.e. the ratcheting rate) and the strain *per unit time* (i.e. the strain rate). Fig. 5 is thus analogous to the relation between strain rate and stress in viscous flow. In general, we write the ratcheting rate law as $\partial\gamma^{\mathrm{p}}/\partial N = f(\tau_{\mathrm{m}})$. The shear stress should be bounded as $\tau_{\mathrm{m}}/Y < 1/\sqrt{3}$; otherwise the film has unlimited plastic shear strain even without the temperature change. As $\tau_{\mathrm{m}}/Y \to 1/\sqrt{3}$, the ratcheting rate becomes large for any given temperature ranges. Depending on the temperature range, we distinguish several behaviors as follows.

When $E_{\mathrm{m}}(\alpha_{\mathrm{m}}-\alpha_{\mathrm{s}})(T_{\mathrm{H}}-T_{\mathrm{L}})/(1-\nu_{\mathrm{m}})Y > 2$, the temperature change by itself can cause the metal film to deform plastically in every cycle. When the shear stress is zero,

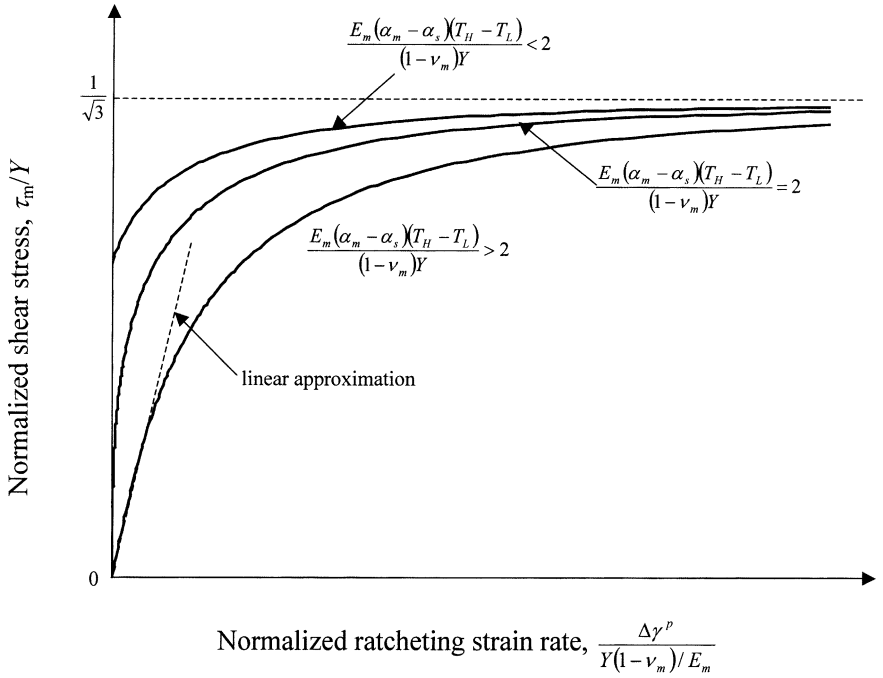

Fig. 5. Shear stress as a function of the ratcheting strain rate.

the metal film undergoes cyclic in-plane plastic deformation, and has no shear strain. When the shear stress is small, the ratcheting rate is linearly proportional to the shear stress:

$$\frac{\partial\gamma^{\mathrm{p}}}{\partial N}=\frac{\tau_{\mathrm{m}}}{\eta}. \tag{13}$$

We call η the ratcheting-viscosity. A comparison between Eqs. (12) and (13) gives

$$\eta=\frac{E_{\mathrm{m}}}{12(1-\nu_{\mathrm{m}})}\left[\frac{E(\alpha_{\mathrm{m}}-\alpha_{\mathrm{s}})(T_{\mathrm{H}}-T_{\mathrm{L}})}{(1-\nu_{\mathrm{m}})Y}-2\right]^{-1}. \tag{14}$$

The linear ratcheting is analogous to the Newtonian viscous flow. The ratcheting-viscosity has the dimension of elastic modulus, and increases when the temperature range decreases. We will mainly use the linear ratcheting approximation (13) in the subsequent development.

When $E_{\mathrm{m}}(\alpha_{\mathrm{m}}-\alpha_{\mathrm{s}})(T_{\mathrm{H}}-T_{\mathrm{L}})/(1-\nu_{\mathrm{m}})Y<2$, the metal film yields only when the shear stress exceeds a critical value, namely, when the quantity in the bracket in Eq. (12) is positive. As seen in Fig. 5, this behavior is analogous to the Bingham viscous flow.

When $E_m(\alpha_m - \alpha_s)(T_H - T_L)/(1 - \nu_m)Y = 2$, for small shear stress, Eq. (12) gives rise to a power law behavior, $\partial\gamma^p/\partial N \sim \tau_m^3$.

3. Ratcheting-creep analogy or cycle-time analogy

This section develops a one-dimensional model of ratcheting of the thin film structures. As shown in Fig. 6, a metal film is in a thick elastic substrate, and the passivation thin film is on the metal film and the substrate. A shear stress, τ_0, due to the packaging substrate, is applied on the passivation film. The shear stress τ_0 is limited by the yield strength of the underfill, on the order 10–100 MPa, and is assumed to be constant during analysis. A variable τ_0 can be incorporated in our model, but will not be incorporated in this paper. The metal film is of thickness h_m and length L. The passivation film is of thickness h_p. Cycle the structure between T_H and T_L. The shear stress in the metal film is τ_m, and the normal stress in the passivation film is σ. Now both τ_m and σ are allowed to vary with the number of cycles, N, and the position, x. We expect τ_m to vary slowly with N and x, so that we will use the ratcheting rate law obtained in the previous section.

First look at the elastic passivation film. As shown in the inset in Fig. 6, the passivation film is subjected to a membrane stress $\sigma(N,x)$, a constant shear stress τ_0 on

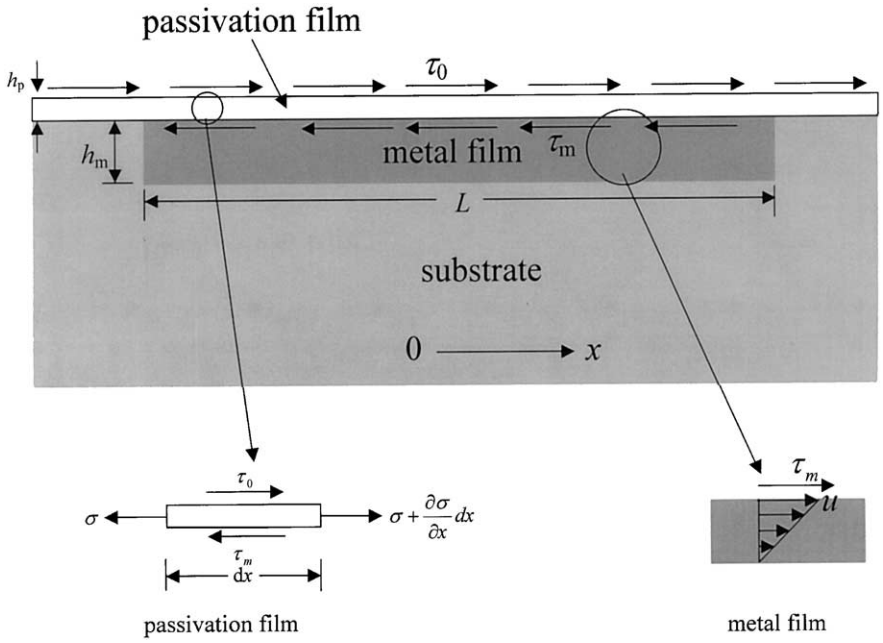

Fig. 6. Illustration of one-dimensional structure of passivation film on the metal film and substrate. The insets show the different element and the stress state of the passivation film, and the stress and flow in the metal film.

the top surface, and a variable shear stress $\tau_m(N,x)$ on the bottom surface. The force balance of the differential element requires that

$$\frac{\partial\sigma}{\partial x}=\frac{\tau_m-\tau_0}{h_p}. \tag{15}$$

Let $u(N,x)$ be the displacement of the passivation film in the x-direction. Elasticity of the passivation film requires that

$$\sigma=E_p\frac{\partial u}{\partial x}, \tag{16}$$

where E_p is Young's modulus of the passivation film.

Next look at the ratcheting metal film. The shear strain relates to the displacement as $\gamma^p=u/h_m$. We assume that the temperature range is large, $E_m(\alpha_m-\alpha_s)(T_H-T_L)/(1-\nu_m)Y>2$.

Consequently, we adopt the shear stress and plastic shear strain increment relation (13) as

$$\tau_m=\eta\frac{\partial u}{h_m\partial N}. \tag{17}$$

The ratcheting-viscosity η is defined by Eq. (14).

Substituting Eqs. (16) and (17) into Eq. (15) gives the governing equation

$$\frac{\partial u}{\partial N}=D\frac{\partial^2 u}{\partial x^2}+\frac{h_m\tau_0}{\eta}. \tag{18}$$

We introduce the ratcheting-diffusivity as

$$D=E_p h_p h_m/\eta. \tag{19}$$

Eq. (18) is a diffusion equation with a source term. A similar equation arises for an elastic film on a viscous layer (Freund and Nix, unpublished work; He et al., 1998).

We assume no separation between the metal film and the substrate, so that the displacement of the metal film at the two edges is the same as the displacement of the substrate. As the substrate is semi-infinite and elastic, its displacement is negligible compared to the accumulated displacement in the passivation film. Consequently, the boundary conditions for the displacement of the passivation film are

$$u=0 \quad \text{at } x=\pm L/2 \quad \text{for all } N. \tag{20}$$

Because the temperature range is large enough to cause the metal to yield in every cycle, so long as there exists a shear stress τ_m in the metal, the metal will ratchet. After many temperature cycles, the structure will reach the steady state, in which the shear stress in the metal film vanishes, $\tau_m=0$, but the cycling temperature still causes the metal film to yield cyclically. The steady state can be obtained by setting $\partial u/\partial N=0$ and satisfying boundary conditions (20). The stress and the displacement of the passivation film in the steady state are given by

$$\sigma=-\frac{\tau_0 x}{h_p}, \quad u=\frac{\tau_0}{2E_p h_p}\left(\frac{L^2}{4}-x^2\right). \tag{21}$$

In the steady state, τ_0 is fully sustained by the membrane stress in the passivation film, giving rise to a linear membrane stress distribution, and a parabolic displacement distribution.

Analogous to any diffusion problem, the characteristic number of cycles to reach the steady state can be estimated by $N_C = L^2/D$, or

$$N_C = \left(\frac{L^2}{h_m h_p}\right) \frac{E_m}{12E_p(1-\nu_m)} \left[\frac{E_m(\alpha_m - \alpha_f)(T_H - T_L)}{(1-\nu_m)Y} - 2\right]^{-1}. \tag{22}$$

The number N_C can be large mainly because the ratio $L^2/(h_m h_p)$ is large. If one replaces the metal film with a plastically deformable polymer, the ratio of elastic modulus of the polymer and the passivation is small, which would significantly reduce N_C. Note that N_C is independent of τ_0.

In order to solve Eq. (18) for evolving stress as the temperature cycles, we need to set the initial condition. Before the temperature cycles, the applied shear stress is balanced by the shear stress in the metal, $\tau_0 \approx \tau_m$, so that the membrane stress in the passivation film is nearly zero, $\sigma \approx 0$, and the initial condition is

$$u = 0 \text{ at } N = 0 \quad \text{for all } x. \tag{23}$$

Using boundary conditions (20) and initial condition (23), we can solve diffusion equation (18). The membrane stress distribution in the passivation film is

$$\sigma = \frac{\tau_0 L}{h_p} \left[\sum_{k=0,1,\ldots} \frac{4(-1)^k}{(2k+1)^2\pi^2} \exp\left[-\frac{(2k+1)^2\pi^2 N}{N_C}\right] \sin\left(\frac{2k+1}{L}\pi x\right) - \frac{x}{L}\right] \tag{24}$$

and the shear stress distribution in the metal film is

$$\tau_m = \tau_0 \sum_{k=0,1,\ldots} \frac{4(-1)^k}{(2k+1)\pi} \exp\left[-\frac{(2k+1)^2\pi^2 N}{N_C}\right] \cos\left(\frac{2k+1}{L}\pi x\right). \tag{25}$$

As the number of thermal cycles increases, the shear stress decreases and the magnitude of the membrane stress increases. When the number of thermal cycles is infinite, the shear stress approaches zero and the normal stress approaches the steady state.

We have made several approximations in this model. The ratcheting strain–stress law (17) is obtained by an analysis of a blanket film under uniform stress. We now allow τ_m to be a function of N and x. Furthermore, the plane strain field is approximated by a shear lag model.

To validate the model, a comparison with the finite element calculation is made. In the finite element calculation, the metal was taken to be elastic and perfectly plastic, with Young's modulus 130 GPa, and yield strength 120 MPa. The substrate and the passivation film were taken to be elastic, with Young's modulus 162 GPa. We took $\tau_0 = 10$ MPa, and the temperature cycle range 165°C. The calculation was done by using the commercial finite element software, ABAQUS, adopting four-node quadrilateral plane strain element. To ensure that the deformation was in the plane strain

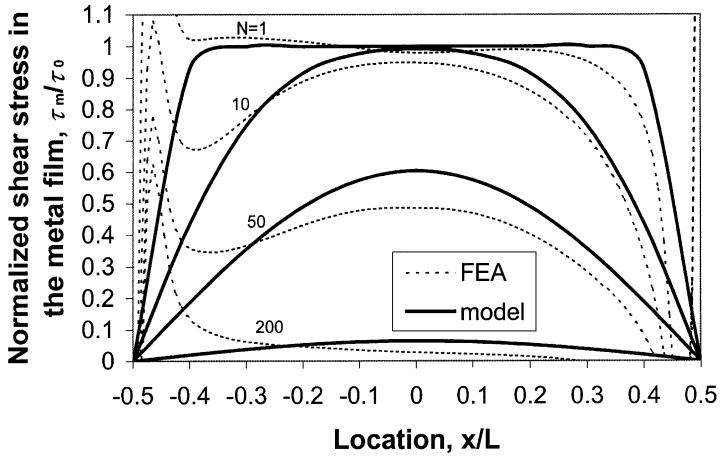

Fig. 7. The normalized shear stress distribution in the metal film for several numbers of thermal cycles.

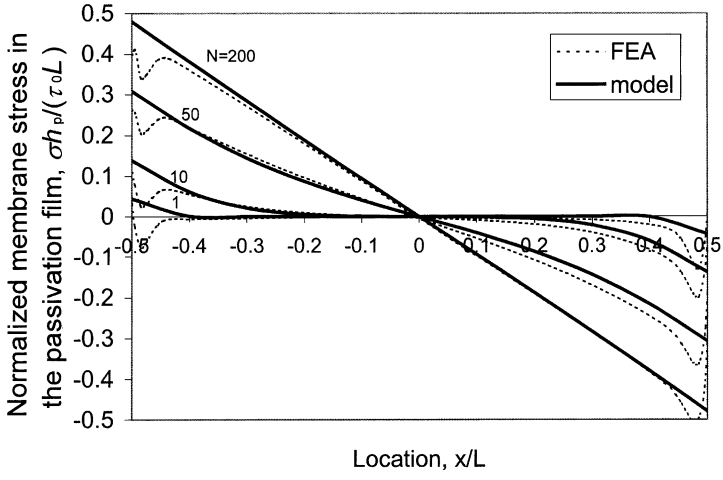

Fig. 8. The normalized membrane stress distribution in the passivation film for several numbers of thermal cycles.

state as the temperature changes, we set the thermal expansion coefficient of the substrate and the passivation film to be zero, and the thermal expansion coefficient of the metal film to be $13 \times 10^{-6}\ \mathrm{K}^{-1}$. The structure is shown in Fig. 2b. The metal film is 100 μm wide and 2 μm thick. The periodic boundary condition is used. Fig. 7 shows the normalized shear stress distribution in the metal film. Fig. 8 shows the normalized membrane stress distribution in the passivation film. Aside from the edges, our model and the FEM calculation predict similar stress distribution and the similar number of cycles to reach the steady state. As expected, the agreement becomes poor near the

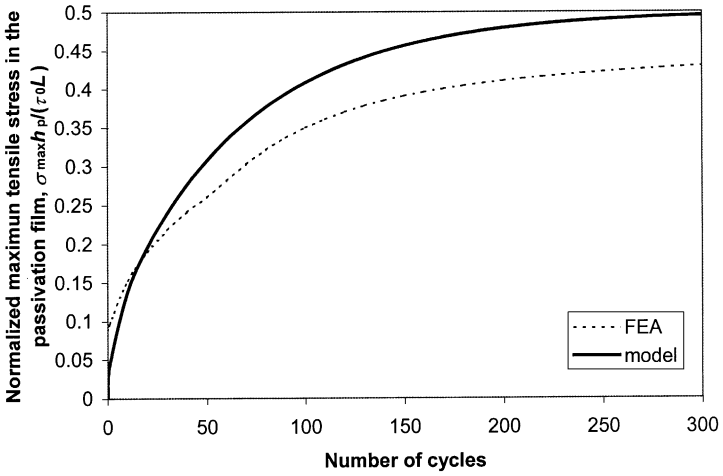

Fig. 9. The normalized maximum tensile stress in the passivation film increases with thermal cycles.

two edges, where the geometric details affect stress concentration. In particular, the maximum tensile stress in the passivation film shows the largest discrepancies. Fig. 9 compares maximum membrane stress calculated from the finite element analysis and that from the model. They show the similar trend. The present model cannot escape from the inherent limitation of the shear lag approximation. Given the simplicity of the present model, however, we believe it should be exploited widely.

4. A two-dimensional model

We now extend the above ideas into a two-dimensional model for the ratcheting of thin film structures. The model is similar to the one for an elastic thin film island on a viscous layer developed by Huang et al. (2001b). Fig. 10 illustrates a metal film encapsulated by a semi-infinite substrate and a passivation film. The thickness of the metal film is small compared to the lateral dimension. The shape of the metal film is arbitrary. As before, we assume that the displacement of the passivation film is zero at the edges.

The passivation film is subject to the membrane stresses σ_{xx}, σ_{xy} and σ_{yy}, the shear stresses τ_{0x} and τ_{0y} on the top surface, and the shear stresses τ_{mx} and τ_{my} on the bottom surface. Force balance of the differential element of the passivation film requires that

$$\frac{\partial \sigma_{xx}}{\partial x} + \frac{\partial \sigma_{xy}}{\partial y} = \frac{\tau_{mx} - \tau_{0x}}{h_{SiN}},$$

$$\frac{\partial \sigma_{xy}}{\partial x} + \frac{\partial \sigma_{yy}}{\partial y} = \frac{\tau_{my} - \tau_{0y}}{h_{SiN}}. \tag{26}$$

As suggested by Eq. (26), the passivation film is in a plane stress condition, the shear stresses on the top and the bottom surfaces acting as the “body force”.

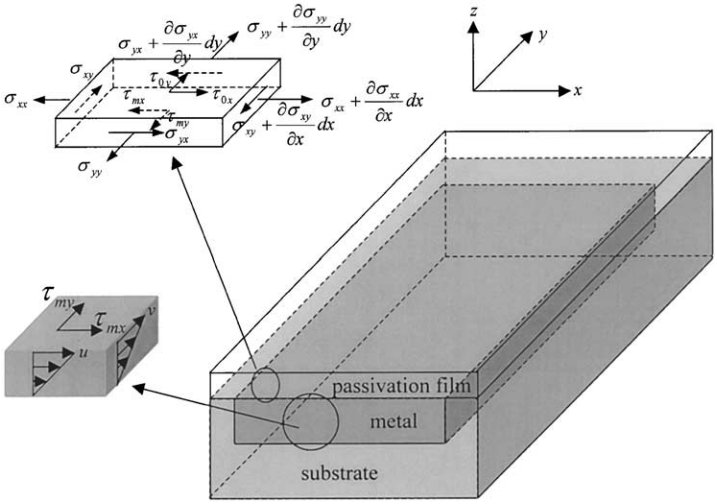

Fig. 10. Illustration of two-dimensional structure of passivation film on the metal film and substrate. The insets show the different element and the stress state of the passivation film, and the stress and flow in the metal film.

Let u and v be the displacement in x- and y-direction, respectively. The strain–displacement relation is

$$\varepsilon_{xx}=\frac{\partial u}{\partial x},\quad \varepsilon_{yy}=\frac{\partial v}{\partial y},\quad \varepsilon_{xy}=\frac{1}{2}\left(\frac{\partial u}{\partial y}+\frac{\partial v}{\partial x}\right). \tag{27}$$

Assuming that the passivation film is isotropic and elastic, the stress–strain relation is

$$\varepsilon_{xx}=\frac{\sigma_{xx}}{E_{\mathrm{p}}}-\nu_{\mathrm{p}}\frac{\sigma_{yy}}{E_{\mathrm{p}}},\quad \varepsilon_{yy}=\frac{\sigma_{yy}}{E_{\mathrm{p}}}-\nu_{\mathrm{p}}\frac{\sigma_{xx}}{E_{\mathrm{p}}},\quad \varepsilon_{xy}=\frac{E_{\mathrm{p}}}{1+\nu_{\mathrm{p}}}\varepsilon_{xy}. \tag{28}$$

The shear stresses on the top surface of the passivation film, τ_{0x} and τ_{0y}, come from the packaging substrate, and are taken to be constant. The shear stresses at the bottom of the passivation film, $\tau_{\mathrm{m}x}$ and $\tau_{\mathrm{m}y}$, come from the metal film, and change as the temperature cycles. Under the shear stress $\tau_{\mathrm{m}x}$ and $\tau_{\mathrm{m}y}$, the metal film ratchets according to

$$\tau_{\mathrm{m}x}=\frac{\eta}{h_{\mathrm{m}}}\frac{\partial u}{\partial N},\quad \tau_{\mathrm{m}y}=\frac{\eta}{h_{\mathrm{m}}}\frac{\partial v}{\partial N}, \tag{29}$$

where the ratcheting-viscosity η is defined by Eq. (14).

Substitution of Eqs. (27)–(29) into Eq. (26) leads to

$$\begin{aligned}\frac{\partial u}{\partial N}&=\frac{D}{(1-\nu_{\mathrm{p}}^2)}\left[\frac{\partial^2 u}{\partial x^2}+\frac{1-\nu_{\mathrm{p}}}{2}\frac{\partial^2 u}{\partial y^2}+\frac{1+\nu_{\mathrm{p}}}{2}\frac{\partial^2 v}{\partial x\partial y}\right]+\frac{h_{\mathrm{m}}\tau_{0x}}{\eta},\\ \frac{\partial v}{\partial N}&=\frac{D}{(1-\nu_{\mathrm{p}}^2)}\left[\frac{\partial^2 v}{\partial y^2}+\frac{1-\nu_{\mathrm{p}}}{2}\frac{\partial^2 v}{\partial x^2}+\frac{1+\nu_{\mathrm{p}}}{2}\frac{\partial^2 u}{\partial x\partial y}\right]+\frac{h_{\mathrm{m}}\tau_{0y}}{\eta}.\end{aligned} \tag{30}$$

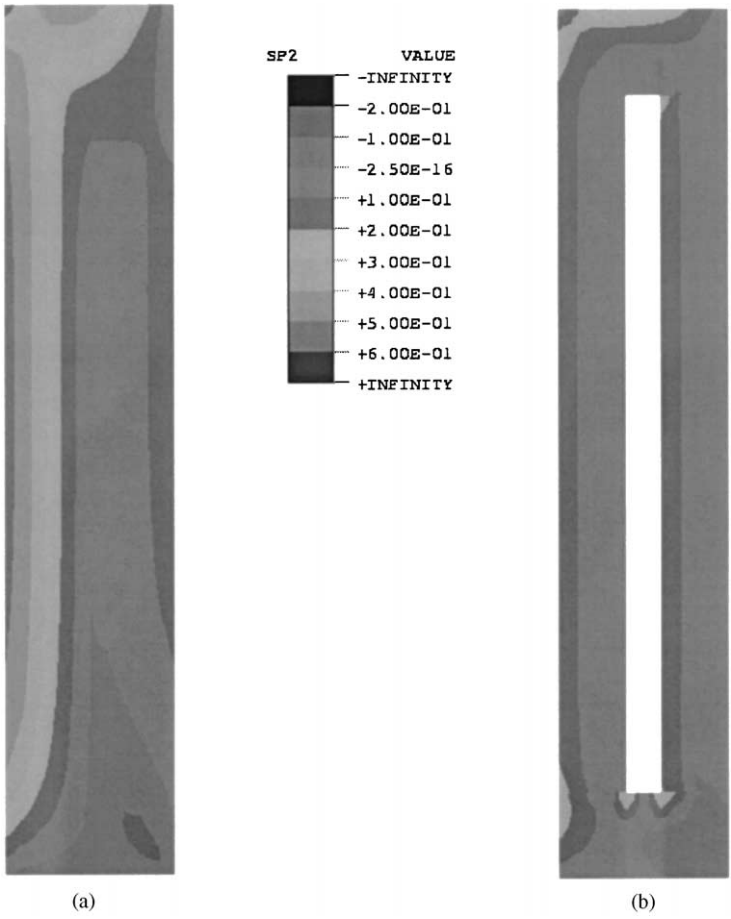

Fig. 11. The normalized maximum principle stress distribution, $(\sigma_{\max} h_p)/(\tau_0 L)$. The length L is taken to be the width of the metal film. (a) A rectangle metal film; (b) a slotted metal film.

The ratcheting-diffusivity, D, is defined by Eq. (19). Eqs. (30) govern the evolution of the displacement field, $u(N,x,y)$ and $v(N,x,y)$. For a given set of boundary and initial conditions, one can calculate the right-hand side (say, by the finite difference method), and then update u and v by an increment ΔN according to Eqs. (30). The procedure is repeated for many steps in the number of cycles. In this paper, we will refrain from presenting any numerical results of the evolution process, and instead focus on the steady state.

In the steady state, the metal film lost the support to the passivation film, $\tau_{mx} = \tau_{my} = 0$. The steady state can be obtained by setting $\partial u/\partial N = 0$ and $\partial v/\partial N = 0$, namely,

$$\frac{\partial^2 u}{\partial x^2} + \frac{1-\nu_p}{2}\frac{\partial^2 u}{\partial y^2} + \frac{1+\nu_p}{2}\frac{\partial^2 v}{\partial x \partial y} = -\frac{(1-\nu_p^2)\tau_{0x}}{E_p h_p},$$

$$\frac{\partial^2 v}{\partial y^2} + \frac{1-\nu_p}{2}\frac{\partial^2 v}{\partial x^2} + \frac{1+\nu_p}{2}\frac{\partial^2 u}{\partial x \partial y} = -\frac{(1-\nu_p^2)\tau_{0y}}{E_p h_p}. \tag{31}$$

By setting the boundary conditions $u = v = 0$ at all edges, Eqs. (31) can be solved by using the finite element method. This is a linear elastic plane stress problem. We have used the commercial finite element software, ABAQUS, adopting four-node quadrilateral plane stress element.

Fig. 11a shows the normalized maximum principal stress distribution at the steady state by applying the uniform shear stress τ_0 in the direction of -45° from the x-axis. The edges of the film are clamped. The size of the film is not important as the membrane stresses in the passivation film scale with $\tau_0 L/h_p$, where L is the width of the metal film. The maximum principal tensile stress is very high near the left edge and the left upper corner, where cracking always happens. One way to reduce the membrane stress is to use a slotted shape. Fig. 11b shows a slotted structure, where the membrane stress in the passivation film is greatly reduced.

The characteristic number of cycles to research the steady state is the same as the one-dimensional model, Eq. (22).

5. Concluding remarks

This paper develops an analytical model to study the stress evolution in the passivation film caused by temperature cycling. The model is based on the analogy between ratcheting and viscous flow. Several approximations are made in this model. By comparing with the finite element calculation, we confirm that the model captures the main features of the problem. The metal film is taken to be a non-hardening material in this model. This corresponds to a safe engineering design, as the hardening metal film can reduce the ratcheting effects (Huang et al., 2001a). The model can also be easily extended to consider the non-linearity of the ratcheting-viscosity by using the finite difference method. The stress concentration at the edges needs to be better treated, as the maximum tensile stress in the passivation film is at the corner. Fracture conditions also need to be considered more carefully (e.g., Liu et al., 2000). Several useful rules for design are evident. First, one should aim to avoid metal film ratcheting altogether. Under cyclic temperature, the metal film cycles elastically if

$$\frac{E_m(\alpha_m - \alpha_s)(T_H - T_L)}{(1-\nu_m)\sqrt{Y^2 - 3\tau_0^2}} < 2. \tag{32}$$

Second, if one cannot avoid ratcheting, one may aim to design the metal film geometry such that the passivation film can sustain the steady state, in which the stress distribution in the passivation film can be calculated by solving a linear elastic plane stress problem. Third, if the characteristic number N_C is much larger than the number of cycles required by the qualification test, one may design according to the transient stress state, solving the stress field as a function of the number of cycles. The present model allows one to evaluate these options in design.

Acknowledgements

The work at Princeton University has been supported by DARPA and Intel Corporation. Discussions with Drs. Jun He and Rowland Cannon are helpful.

References

Alpern, P., Wicher, V., Tilgner, R., 1994. A simple test chip to assess chip and package design in the case of plastic assembling. IEEE Trans. Compon. Pack. Manuf. Technol. A 17, 583–589 (correction in 1995, 18, 862–863).

Begley, M.R., Evans, A.G., 2001. Progressive cracking of a multi-layer system upon thermal cycling. ASME Trans. J. Appl. Mech. 68 (4), 513–520.

Bree, J., 1967. Elastic–plastic behaviour of thin tubes subjected to internal pressure and intermittent high-heat fluxes with application to fast-nuclear-reactor fuel elements. J. Strain Analysis 2, 226–238.

Edwards, D.R., Heinen, K.G., Groothuis, S.K., Martinez, J.E., 1987. Shear-stress evaluation of plastic packages. IEEE Trans. Compon. Hybrids Manuf. Technol. 12 (4), 618–627.

Gee, S.A., Johnson, M.R., Chen, K.L., 1995. A test chip design for detecting thin-film cracking in integrated-circuits. IEEE Trans. Compon. Pack. Manuf. Technol. B 18 (3), 478–484.

Gurumurthy, C.K., Jiao, J., Norris, L.G., Hui, C.-Y., Kramer, E.J., 1998. A thermo-mechanical approach for fatigue testing of polymer bimaterial interfaces. ASME Trans. J. Electron. Pack. 120 (4), 372–378.

He, J., Shaw, M.C., Sridhar, N., Cox, B.N., Clarke, D.R., 1998. Direct measurements of thermal stress distributions in large die bonds for power electronics. MRS Symp. Proc. 515, 99–104.

He, M.Y., Evans, A.G., Hutchinson, J.W., 2000. The ratcheting of compressed thermally grown thin films on ductile substrates. Acta Mater. 48 (10), 2593–2601.

Hill, R., 1950. The Mathematical Theory of Plasticity. Clarendon Press, Oxford.

Huang, M., Suo, Z., Ma, Q., 2001a. Metal film crawling in interconnected structures caused by cyclic temperatures. Acta Mater. 49 (15), 3039–3049.

Huang, M., Suo, Z., Ma, Q., Fujimoto, H., 2000. Thin film cracking and ratcheting caused by temperature cycling. J. Mater. Res. 15 (6), 1239–1242.

Huang, R., Yin, H., Suo, Z., Sturm, J.C., Hobart, K.D., 2001b. Stress relaxation of a thin film island on a viscous substrate. Unpublished work.

Isagawa, M., Iwasaki, Y., Sutoh, T., 1980. Deformation of Al metallization in plastic encapsulated semiconductor devices caused by thermal shock. Proceedings of the International Reliability Physics Symposium, 171–177.

Jansson, S., Leckie, F.A., 1992. Mechanical-behavior of a continuous fiber-reinforced aluminum matrix composite subjected to transverse and thermal loading. J. Mech. Phys. Solids 40 (3), 593–612.

Karlsson, A.M., Evans, A.G., 2001. A numerical model for the cyclic instability of thermally grown oxides in thermal barrier systems. Acta Mater. 49 (10), 1793–1804.

Lau, J., Wong, C.P., Prince, J.L., Nakayama, W., 1998. Electronic Packaging, Design, Materials, Process, and Reliability. McGraw-Hill, New York.

Liu, X.H., Suo, Z., Ma, Q., 1999. Split singularities: stress field near the edge of a silicon die on a polymer substrate. Acta Mater. 47 (1), 67–76.

Liu, X.H., Suo, Z., Ma, Q., Fujimoto, H., 2000. Developing design rules to avert cracking and debonding in integrated circuit structures. Eng. Fracture Mech. 66, 387–402.

Ma, Q., Xie, J., Chao, S., El-Mansy, S., McFadden, R., Fujimoto, H., 1998. Channel cracking technique for toughness measurement of brittle dielectric thin films on silicon substrates. In: Bravman, J.C., Marieb, T.N., Lloyd, J.R., Korhonen, M.A. (Eds.), Materials Reliability in Microelectronics VIII, Materials Research Society, Pittsburgh, p. 331.

Michaelides, S., Sitaraman, S.K., 1999. Die cracking and reliable die design for flip-chip assemblies. IEEE Trans. Adv. Pack. 22 (4), 602–613.

Nguyen, L.T., Gee, S.A., Johnson, M.R., Grimm, H.E., Berardi, H., Walberg, R.L., 1995. Effects of die coatings, mold compounds, and test conditions on temperature cycling failures. IEEE Trans. Compon. Pack. Manuf. Technol. A 18 (1), 15–22.

Nix, W.D., 1989. Mechanical-properties of thin-films. Metall. Trans. 20A, 2217–2245.
Pendse, R.D., 1991. A comprehensive approach for the analysis of package induced stress in ICs using analytical and empirical-methods. IEEE Trans. Compon. Hybrids Manuf. Technol. 14 (4), 870–873.
Suresh, S., 1998. Fatigue of Materials, 2nd Edition. Cambridge University Press, Cambridge.
Thomas, R.E., 1985. Stress-induced deformation of aluminum metallization in plastic molded semiconductor-devices. IEEE Trans. Compon. Hybrids Manuf. Technol. 8 (4), 427–434.
Yan, X., Agarwal, R.K., 1998. Two test specimens for determining the interfacial fracture toughness in flip-chip assemblies. ASME Trans. J. Electron. Pack. 120 (2), 150–155.